Computers & Geosciences 59 (2013) 132–147

Contents lists available at SciVerse ScienceDirect

Computers & Geosciences

journal homepage: www.elsevier.com/locate/cageo

Watershed delineation from the medial axis of river networks

Farid Karimipour [a,*], Mehran Ghandehari [a], Hugo Ledoux [b]

[a] Department of Surveying and Geomatics Engineering, College of Engineering, University of Tehran, Tehran, Iran
[b] Delft University of Technology, The Netherlands

ARTICLE INFO

Article history:
Received 31 December 2012
Received in revised form
10 June 2013
Accepted 12 June 2013
Available online 20 June 2013

Keywords:
Watersheds
Medial axis
Voronoi diagram
Delaunay triangulation
River network

ABSTRACT

The watersheds are commonly delineated from digital elevation models (DEM). This approach is not efficient when an accurate DEM is not available. Furthermore, since raster-based algorithms are employed, the computations for large areas are very time consuming and even may be impractical. This article investigates delineation of the watersheds from the medial axis of river networks: If the river network is sampled by a set of points, the medial axis of the sample points provides an approximation of the catchments, whose aggregation results in the watersheds. Although this idea has been already proposed in the literature, the complexities of the medial axis extraction prevent it from being practically used. A major issue is appearing extraneous branches in the media axis due to perturbations of the sample points, which must be filtered out in a pre- or post-processing step. This article improves a Voronoi-based medial axis extraction algorithm by using labeled sample points to automatically avoid extraneous branches. The proposed method is used in four case studies to delineate the watersheds. The results illustrate that the proposed method is stable, easy to implement and robust, even in presence of significant noises and perturbations. The results also indicate that the watersheds delineated using the proposed and the DEM-based methods are reasonably comparable.

1. Introduction

A watershed (also called drainage area or basin) is a hydrological unit where precipitations that fall into this area, eventually end up in the same particular point (called outlet or pour point). This structure is the basis for a variety of hydrological geo-analysis (McAllister, 1999). The watershed may be manually delineated through connecting the mountains' peak to the maxima of the contour lines. The result is affected by the contour lines' accuracy and interval, which depend on the accuracy and density of the sample points, per se. Trivial errors are also unavoidable, especially for flat terrains and large areas (Al-Muqdadi and Merkel, 2011). Nowadays, improved processing power of computers and access to new terrain surface models has led to automatic watershed delineation techniques, which are faster and more precise (Martz and Garbrecht, 1992).

The raster-based algorithms, which usually use the digital elevation models (DEM), are very common in automatic watershed delineation (Chorowicz et al., 1992; Jones et al., 1990; Lin et al., 2006; Mark, 1984; Martz and Garbrecht, 1992, 1993; Mower, 1994; Nelson et al., 1994; Tarboton, 1997; Turcotte et al., 2001; Yang et al., 2010). Assuming that water always flows along the path of the steepest descent, DEM-based methods simulate the rainfall and extract the cells whose precipitations eventually end up into the same particular point (i.e., the definition of the watershed).

The DEM-based methods have some difficulties: (1) The raster computations for large areas are very time consuming and even may be impractical; (2) the accuracy of these methods depends on the quality and type of the DEM used, which is, per se, affected by the accuracy, density and distribution of the source data, the smoothness of the terrain surface and the deployed interpolation method (Li et al., 2005); (3) the flow path is restricted to the grid axes and the water is trapped in sinks and flat areas due to limitations in flow direction computation; and (4) the raster to vector conversion of the boundaries may results in creating twisted polygons, i.e., two polygons connected only at one point are considered as single polygon (Fig. 1).

On top of these, the river network may be the only available data in some cases, where an accurate DEM is not available. In this situation, the best approximation of the watersheds would be to extract the region that is closer to each river segment than to any other (called the river catchments) and aggregate the catchments of the rivers fall into the same main river (Dillabaugh, 2002; Gold and Dakowicz, 2005; McAllister, 1999). This approximation is obtained through the medial axis (MA) extraction, which is defined as the set of points that are equidistant from at least two points on the boundary of the shape.

* Corresponding author. Tel.: +98 21 61114376; fax: +98 21 88008841.
E-mail addresses: fkarimipr@ut.ac.ir, karimipour@geoinfo.tuwien.ac.at (F. Karimipour), ghandehary@ut.ac.ir (M. Ghandehari), h.ledoux@tudelft.nl (H. Ledoux).

0098-3004/$ - see front matter © 2013 Elsevier Ltd. All rights reserved.
http://dx.doi.org/10.1016/j.cageo.2013.06.004

Fig. 1. Twisted polygons issue in DEM-based methods: In each figure, the polygons pointed by arrows are twisted, i.e., they intersect themselves.

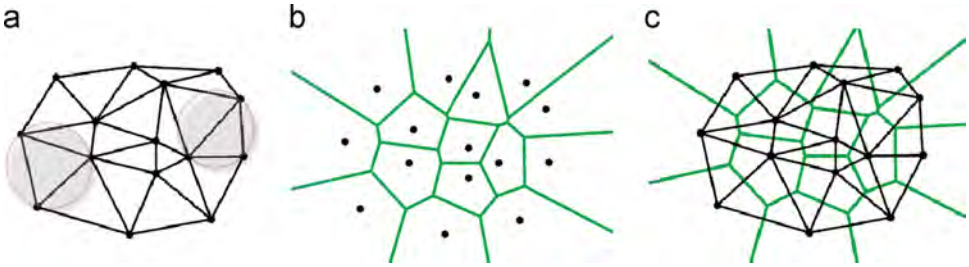

Fig. 2. (a) Delaunay triangulation; (b) Voronoi diagram; (c) Duality of DT and VD.

This article aims to verify the hypothesis stated by Gold and Snoeyink (2001) that uses a Voronoi-based MA extraction method (called one-step crust and skeleton algorithm) for the watershed delineation: The river network is sampled by a set of points, and Delaunay triangulation and Voronoi diagrams are used to extract the MA, which results in an approximation of the watersheds. The initial investigations of applying the method to a small dataset show that this method gives a fair approximation of the watersheds, but it has never been practically evaluated (Gold and Dakowicz, 2005). Furthermore, there are some issues with the one-step crust and skeleton algorithm to be solved in order to be practically used for the watershed delineation from river networks: (1) The original curves (the rivers, here) may not be correctly reconstructed at sharp corners due to poor distribution of points, resulting the MAs to break through the rivers, which must be manually edited by the user; (2) the algorithm is designed to extract the MA of closed curves, which is not the case with the river networks. Thus, Applying the MA extraction algorithm to river networks does not produce the expected results in some cases, which must be edited by the user; (3) the MA extraction of river networks does not necessarily produce a closed polygon (as the catchment) for each river, and a post-processing user check is needed to manually close the polygons; and (4) the MA is very sensitive to small changes of the boundary, so it is instable under small boundary perturbations, results in many irrelevant branches in the MA (the catchments, here), which must be filtered out in a pre- or post-processing step.

This article proposes an improvement to the one-step crust and skeleton algorithm to solve the above issues in watershed delineation through labeling the sample points. All of the sample points corresponding to each river segment (which are the sections naturally defined by branchings and confluences of rivers) are assigned the same label. Furthermore, we propose automatic procedures to modify the MA at sharp corners as well as to construct the watershed polygons from the extracted MA (which is only a set of lines). The conceptual structure and the implementation results illustrate that the proposed method is stable, easy to implement and robust, even in the presence of significant noise and perturbations, able to handle sharp corners and open curves and guarantees producing one polygon per catchment.

The rest of the article is organized as follows: Section 2 represents some geometric preliminaries, including Delaunay triangulation, Voronoi diagram and medial axis. Section 3, introduces the one-step crust and skeleton algorithm to extract the MA, and reviews the methods proposed in the literature to filter the extraneous MA branches. In Section 4, we present the proposed improvement to the one-step crust and skeleton algorithm and explain how it solves the issues of this algorithm in order to be practically used for watershed delineation. The results of using the proposed method in four case studies are presented and evaluated in Section 5. The results are also compared with the watersheds delineated through a DEM-based method. Finally, Section 6 contains concluding remarks and ideas for future work.

2. Geometric preliminaries

This section contains some geometric preliminaries, including Delaunay triangulation, Voronoi diagram and medial axis. In this section, $\mathcal{O}$ is a 2D object and $\partial\mathcal{O}$ is its boundary.

2.1. Delaunay triangulation

Definition 1. Given a point set S in the plane, a triangulation of the points in S is *Delaunay if it* satisfies the circum-circle property: The circle passes through three vertices of each triangle (called circum-circle) does not contain any other point $s \in S$ (Karimipour et al., 2010; Okabe et al., 2000) (Fig. 2a). In other words, any three points uniquely define a circle. Given a set of points connected such that every point is part of a triangle, this set of triangles is a Delaunay triangulation if the circle defined by each triangle has no points in its interior.

2.2. Voronoi diagram

Definition 2. Let S be a set of points in R^2. The Voronoi diagrams of the point set S, denoted as $VD(S)$ is a partitioning of the space where each $p_i \in S$ is assigned a cell C_i so that all points $q \in C_i$ are closer to p_i than any other $p_j \in S$ (Karimipour et al., 2010; Okabe et al., 2000) (Fig. 2b).

For Voronoi diagram of sample points S, the Voronoi vertices are classified into *inner* and *outer vertices*, which lie inside and outside $\mathcal{O}$, respectively. Then, the Voronoi edges are classified into three groups: edges connecting two inner vertices (*inner Voronoi edges*), edges connecting two outer vertices (*outer Voronoi edges*),

and edges connecting an inner and an outer vertices (*mixed Voronoi edges*).

Delaunay triangulation and Voronoi diagrams are dual structures. This means that each node in Delaunay triangulation corresponds to a Voronoi cell, each Delaunay edge corresponds to a Voronoi edge and each Delaunay triangle corresponds to a Voronoi vertex. The centers of circum-circles of Delaunay triangulation are the Voronoi vertexes; and joining the adjacent generator points in Voronoi diagram yields their Delaunay triangulation (Fig. 2c). This duality is very useful because construction, manipulation and storage of the Voronoi diagram are more difficult than Delaunay triangulation, so all the operations can be performed on Delaunay triangulation, and the Voronoi diagram is only extracted on demand (Ledoux, 2006).

Delaunay triangulation and Voronoi diagrams are well known in geosciences for many years (Mostafavi et al., 2003). They are the basic data structures for many geoscientific applications such as terrain modeling, spatial interpolation and geological mapping problem. Here, we use them to reconstruct the crust of objects sampled at some finite locations (Aurenhammer, 1991; Delaunay, 1934; Ledoux and Gold, 2007) as well as the basis for extraction of the medial axis.

2.3. Medial axis

The medial axis (also called crust) was first introduced by Blum et al. (1967) as a tool in image analysis. Grassfire model is the most popular definition of the MA with an intuitive concept: Consider starting a fire on the boundary of a shape in the plane. The fire starts at the same moment, everywhere on the boundary and it propagates with homogeneous velocity in every directions. The MA is the set of points where the front of the fire collides with itself, or other fire front. Mathematically:

Definition 3. The *medial axis* is (the closure of) the set of points in $\mathcal{O}$ that have at least two closest points on the object's boundary $\partial\mathcal{O}$ (Amenta et al., 1998).

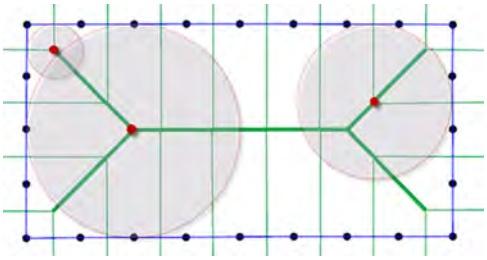

Fig. 3. The MA (green line) of a 2D curve (rectangle). (For interpretation of the references to color in this figure legend, the reader is referred to the web version of this article.)

Another description defines the MA as the centers of the set of maximal disks contained in $\mathcal{O}$ (a maximal disk is a disk contained in a shape that is not completely covered by another disk contained in the shape) (Fig. 3).

The *skeleton* is a concept closely related to the MA. Some literatures consider the skeleton equivalent to the MA (Gonzalez and Woods, 2002), while some others believe they are similar, but are not equal (Russ, 2002). In this article, we consider both the MA and the skeleton as equal terms and use the terms, interchangeably.

3. Voronoi-based medial axis extraction

Several Voronoi-based algorithms have been proposed in the literature for the medial axis extraction, including Voronoi ball algorithm (Amenta et al., 2001; Amenta and Kolluri, 2001), Voronoi edge algorithm (Attali and Montanvert, 1997), crust algorithm (Amenta et al., 1998). In this paper, we focus on an algorithm called "one-step crust and skeleton algorithm" (Gold and Snoeyink, 2001), which is simpler and simultaneously reconstructs the curve and extracts the MA in fewer step (Karimipour and Ghandehari, 2013). We explain this algorithm and improve it later for the watershed delineation.

3.1. One-step crust and skeleton algorithm

Amenta et al. (1998) proposed a Voronoi-based algorithm (called crust algorithm) to reconstruct the boundary of a shape from a set of sample points. Gold and Snoeyink (2001) improved this algorithm so that both the boundary (crust) and the MA (skeleton) are extracted, simultaneously, and the coined the name "one-step crust and skeleton" for this algorithm. We call it OSCS algorithm, hereafter.

In the OSCS algorithm, crust/skeleton is a subset of Voronoi/Delaunay edges. The inclusion of an edge in the structure is determined by a simple *inCircle* test. Each Delaunay edge (D_1D_2 in Fig. 4a) belongs to two triangles ($D_1D_2D_3$ and $D_1D_2D_4$ in Fig. 4a). For each Delaunay edge, there is a dual Voronoi edge (V_1V_2 in Fig. 4a). Suppose two triangles $D_1D_2D_3$ and $D_1D_2D_4$ have a common edge D_1D_2 whose dual Voronoi edge is V_1V_2. The *InCircle* (D_1, D_2, V_1, V_2) determines the position of V_2 respect to the circle passes through D_1, D_2 and V_1. If V_2 is outside the circle, D_1D_2 belongs to the crust (Fig. 4b); otherwise, if V_2 is inside, V_1V_2 belongs to the skeleton (Fig. 4c). The value of *InCircle* (D_1, D_2, V_1, V_2) test is calculated using the following determinant:

$$InCircle\ (D_1,D_2,V_1,V_2)=\begin{bmatrix} xD1 & yD1 & xD1^2+yD1^2 & 1\\ xD2 & yD2 & x2^2+yD2^2 & 1\\ xV1 & yV1 & xV1^2+yV1^2 & 1\\ xV2 & yV2 & xV2^2+V2^2 & 1 \end{bmatrix} \quad (1)$$

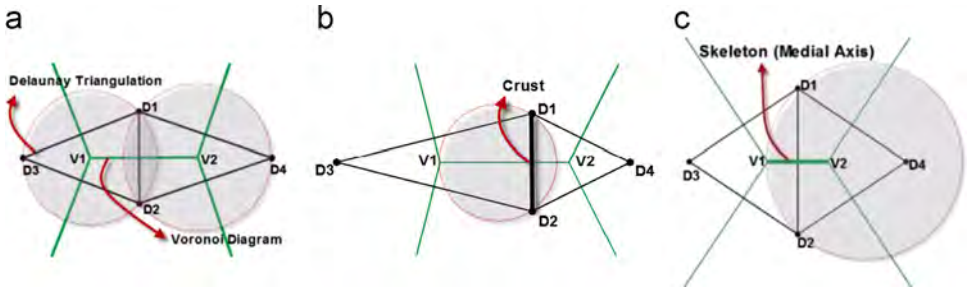

Fig. 4. One-step crust and skeleton algorithm: (a) Delaunay triangulation and Voronoi diagram of four sample points D_1 to D_4; (b) V_2 is outside the circle passes through D_1, D_2 and V_1, so D_1D_2 belongs to the crust; (c) V_2 is inside the circle passes through D_1, D_2 and V_1, so V_1V_2 belongs to the skeleton.

If (D_1, D_2, V_1) is clockwise, then D_1D_2 belongs to the crust if this determinant is negative, otherwise V_1V_2 belongs to the skeleton (Gold and Snoeyink, 2001; Karimipour et al., 2008).

The pseudo-code of the OSCS algorithm is as follows:

One-step crust and skeleton extraction

Input: Set of sample points S
Output: Crust and skeleton of the shape approximated by S

1. DT←Delaunay triangulation of S
2. E←Edges of DT
3. For every $e \in E$ do
4. S_1, S_2 ←Triangles that have e as an edge
5. D_1, D_2 ←End points of e
6. V_1, V_2 ←Centers of the circum-circles of S_1 and S_2 and (D_1, D_2, V_1) is CW
7. H ←*InCircle* (D_1, D_2, V_1, V_2)
8. If $H < 0$ then $D_1D_2 \in$ Crust
9. else $V_1V_2 \in$ Skeleton

Fig. 5. MA extraction of a river network yields an approximation of the watersheds, but many extraneous edges exist.

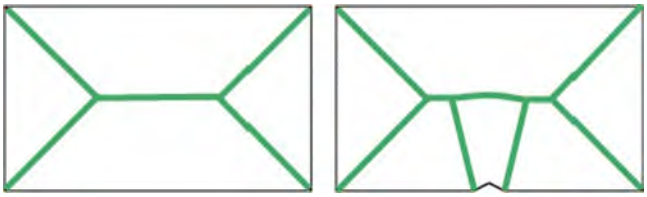

Fig. 6. Similar shapes may have significantly different MAs due to boundary perturbations.

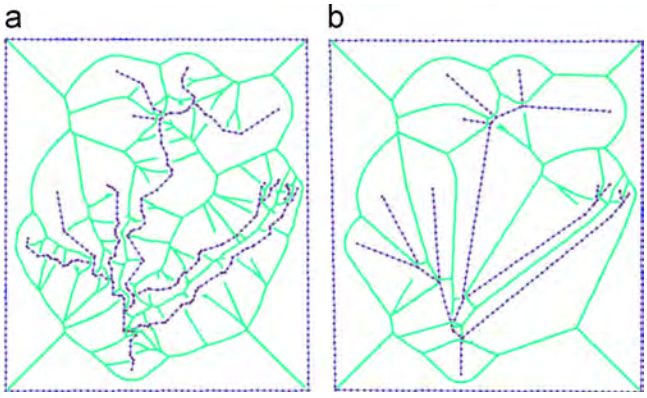

Fig. 7. MA approximation of a river network: (a) before and (b) after simplification.

As illustrated in Fig. 5, if the OSCS algorithm is applied to a river network, the extracted MA yields a fair approximation of the corresponding watersheds. However, the extracted MA will generally contain many extraneous branches due to small perturbations of the sample points. These must be filtered out. In the following, we review existing filtering methods, as well as their problems. We then present an improved method which avoids the problem altogether.

3.2. Filtering the extraneous edges in the medial axis

The MA is inherently unstable under small perturbations; i.e., it is very sensitive to the small changes of the boundary, which produce many extraneous branches in the MA. As a result, two similar shapes may have significantly different MAs (Fig. 6). Filtering extraneous branches is a common approach to extract

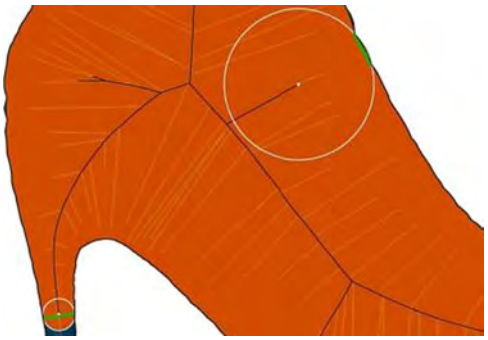

Fig. 8. Importance values assigned by λ-medial axis method (Miklós, 2012).

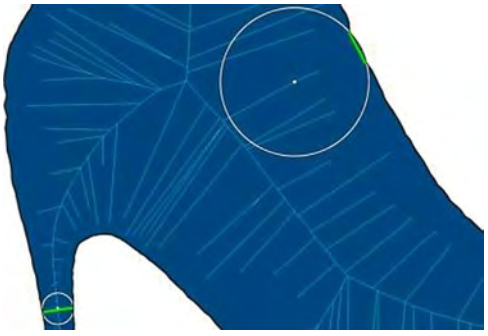

Fig. 9. Importance values assigned by angle filtration (Miklós, 2012).

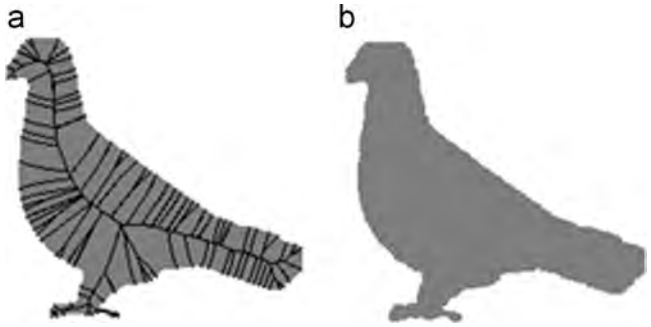

Fig. 10. Shape reconstruction from the MA: (a) Original shape and its MA; (b) the shape reconstructed from the MA (Bai and Latecki, 2007).

the major parts of the MA. Such filtering may be applied as pre-processing through simplifying (smoothing) the boundary, or as post-processing through pruning that eliminate the extraneous branches of the extracted MA.

3.2.1. Simplification

Some of the filtering methods simplify the boundary before computing the MA by removing perturbations or boundary noises (Fig. 7) (Attali and Montanvert, 1996; Siddiqi et al., 2002). Although these methods aim to remove unwanted boundary noises, they may not provide the ideal results: (1) The distinction between boundary data and noise is difficult; (2) some extraneous edges may remain in the filtered MA; and (3) these methods can alter the topological structure and thus the MA position.

3.2.2. Pruning

The purpose of the pruning algorithms, as a post-processing step is to remove irrelevant branches in order to preserve only the significant parts of the MA. Different criteria were proposed in such algorithms to assign an *importance value* to each branch, and then branches with the importance values less than a given threshold are removed (Attali et al., 1995; Attali and Montanvert, 1994; Bai and Latecki, 2007; Chazal and Lieutier, 2005; Giesen et al., 2009; Malandain and Fernández-Vidal, 1998; Ogniewicz and Kübler, 1995). Typically, these criteria are based on angle, distance, area, etc.

Pruning algorithms have some drawbacks; (1) Some irrelevant branches may not be eliminated entirely; (2) eliminating irrelevant branches usually shorten the main branches as well; (3) a disconnection in the main structure of the MA may occur; (4) many of the pruning methods cannot preserve the topology of a complex shape; and (5) in some cases, multiple parameters are required and, for which it is difficult to determine appropriate thresholds, simultaneously. On top of these, pruning methods need user checks at the end.

3.2.2.1. λ-Medial axis. Chazal and Lieutier (2005) introduced the λ-medial axis pruning method. As Fig. 8 shows, they assign the importance values based on the distance between the contact points (i.e., the points where a Voronoi ball touches the shape's boundary). They showed that the λ-medial axis preserves topology for a restricted range of values of λ and proved geometric stability with respect to small perturbations. However, λ is a global threshold and does not adopt the local size of the object. For example in Fig. 8, by applying a global threshold, the MA branches corresponding to the two circles have been removed, while the MA branch of the small circle should have been remained.

3.2.2.2. Angle filtration. Attali and Montanvert (1994) proposed an algorithm to prune the MA using an angular parameter. This angle is the maximum angle formed by the MA end point, and its corresponding contact points (Fig. 9). They observed that the vertices of irrelevant branches from smaller bisector angles. This method does not guarantee the stability and its threshold depends on the distribution of sample points. For example, in Fig. 9, the MA branch corresponding to the large circle is correctly removed, while the MA branch of the small circle is mistakenly pruned out because of poor sample point distribution.

3.2.2.3. Discrete skeleton evolution. Bai and Latecki (2007) introduced the discrete skeleton evolution as an area-based pruning method. The threshold is defined based on the difference between the area of initial shape and the shape reconstructed from the simplified skeleton (Fig. 10). This method considers a weight w_i for each end branch, which is an edge of skeleton that has one junction point:

$$w_i = \frac{A(R(S-P(L_i)))-1}{A(R(S))} \quad (2)$$

where A is area function, S is the original skeleton, $P(L_i)$ is an end branch and $R(S)$ is the shape reconstructed from the skeleton.

Generally, an end branch with a small weight w_i has a little influence on the reconstruction, since the area of the reconstruction without this branch is nearly the same as the area of the reconstruction with it, so it can be safely removed (Bai and Latecki,

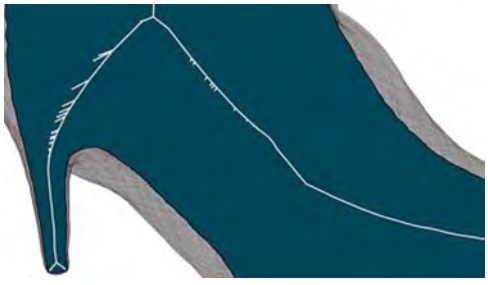

Fig. 13. Tiny extraneous branches in the MA after using the scale axis transform algorithm (Giesen et al., 2009).

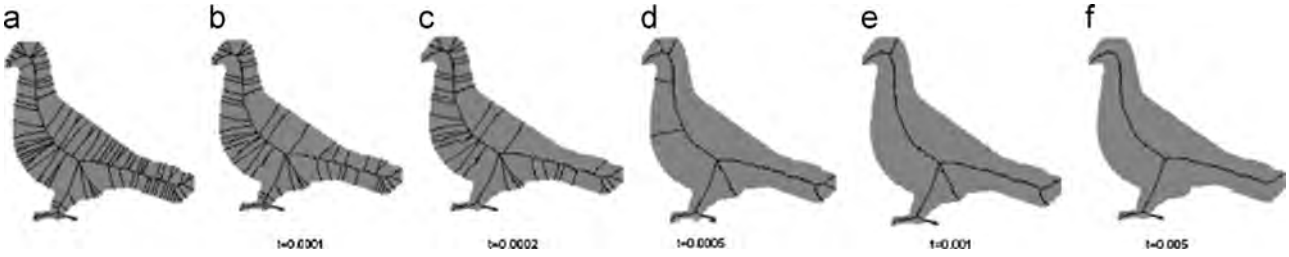

Fig. 11. The discrete skeleton evolution algorithm: (a) The original skeleton; (b)–(f) the pruned skeletons with different thresholds (Bai and Latecki, 2007).

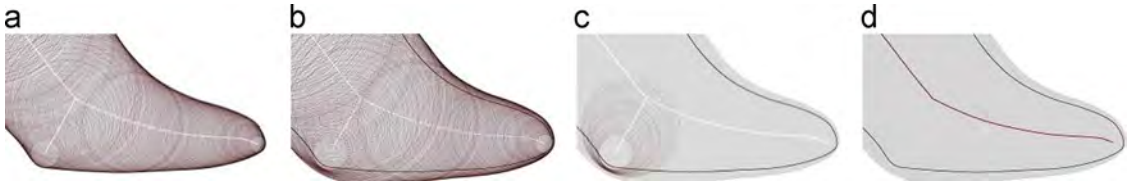

Fig. 12. The steps of the scale axis transform algorithm: (a) The original MA and the inner Voronoi balls; (b) the radius of Voronoi balls is multiplied by a multiplicative scaling factor; (c) small balls are covered by larger balls; (d) the MA of the grown shape (Giesen et al., 2009).

2007). Fig. 11 shows the results of this algorithm for different thresholds. This method shortens the main branches. Furthermore, finding an appropriate threshold is difficult.

3.2.2.4. Scale axis transform. In the λ-medial axis method, some main branches of the MA may be eliminated, because the radii of their corresponding balls are smaller than the threshold. Replacing the global parameter for the whole shape with local parameters for each part of the shape is a solution to deal with this issue.

Giesen et al. (2009) presented a different method called scale axis transform. They multiply the radius of all inner Voronoi balls by a certain simplification factor and consider their union as the grown shape. Then, the MA of the grown shape is considered as the simplified MA. Fig. 12 illustrates the steps of this method. The radius of the Voronoi balls is multiplied by a coefficient (multiplicative scaling) (Fig. 12b). The Voronoi balls correspond to less important branches are covered by larger balls (Fig. 12c) and therefore small balls are eliminated. Thus, the MA of the grown shape keeps the whole main branches (Fig. 12d). Although deploying local thresholds

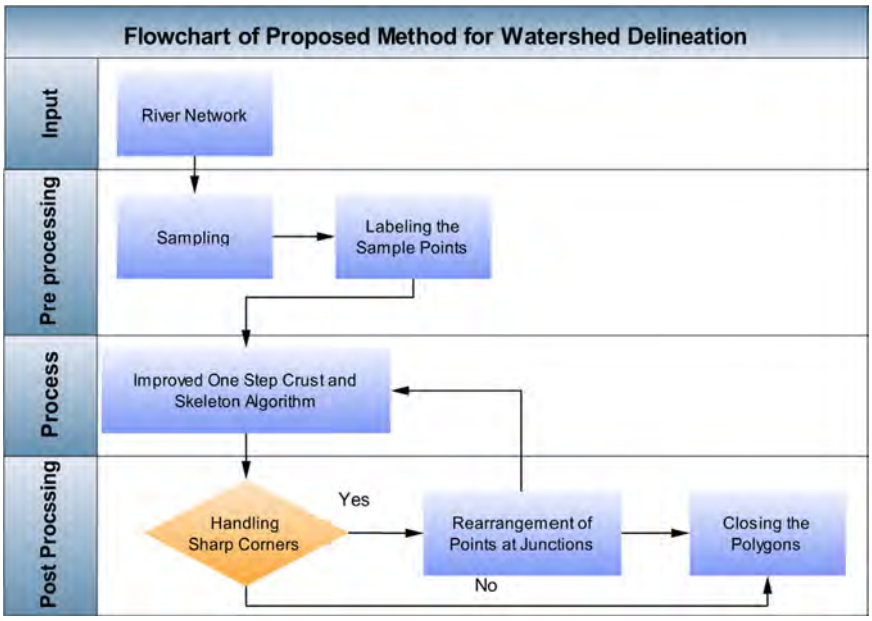

Fig.14. The flowchart of the proposed method for watershed delineation.

Fig. 15. Different definition of junctions (red points) result in different MAs: The more junctions, the more branches in the MA. (For interpretation of the references to color in this figure legend, the reader is referred to the web version of this article.)

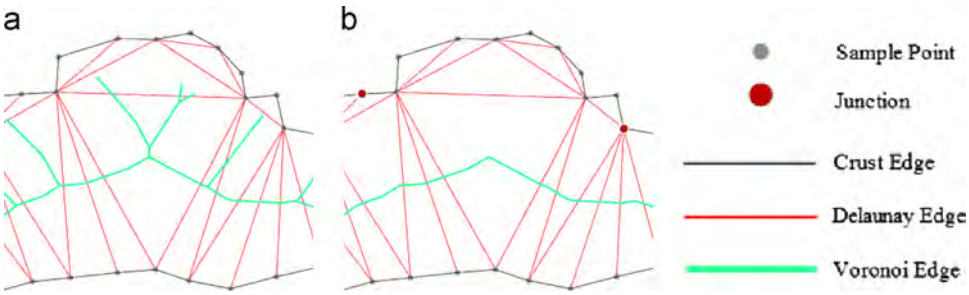

Fig. 16. (a) OSCS algorithm detects some extraneous edges as parts of the MA. They are the Voronoi edges created between the sample points that lie on the same segment of the curve; (b) the improved method automatically avoid such edges in the MA.

is an advantage, the result of this method may still contain some tiny extraneous branches (Fig. 13).

4. Proposed method for watershed delineation using the medial axis

This section explains the proposed method of the article for watershed delineation from river networks. The core of the approach is an improvement we made in the one-step crust and skeleton algorithm to solve the issues mentioned in Section 1 in order to be practically used for watershed delineation from river networks. The procedure of the watershed delineation using the proposed method is as follows (Fig. 14):

4.1. Sampling

The river networks are approximated by sampling. If sampling is sufficiently dense, the sample points carry the shape information of the river, i.e., they can be used to reconstruct the original river and approximate its MA. The quality of sample points S has a direct effect on reconstructing the river and approximating the MA. Several theoretical criteria have been proposed in the literature for a proper sampling (Amenta et al., 1998). However, they may not be useful in practice. For instance, from a theoretical point of view, for sharp corners and noisy samples, infinite dense sampling is needed to guarantee the proper reconstruction, which is not practically possible (Cheng et al., 2005; Dey and Wenger, 2002).

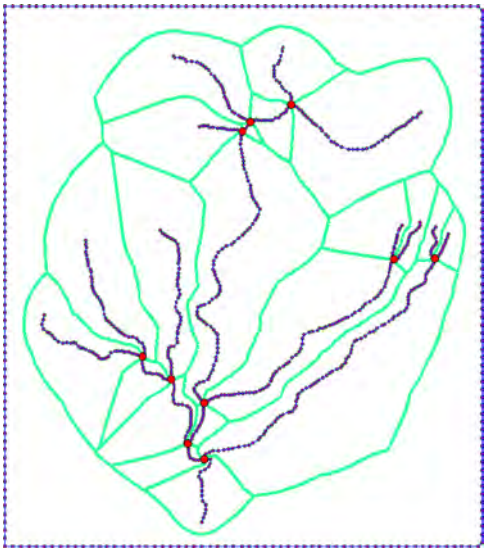

Fig. 17. MA extraction of a river network using the proposed method automatically avoids appearing the extraneous branches in the MA.

In practice, sampling is performed manually so that the sample points fairly approximate the curve. This process cannot be fully automatic due to the fact that intersection of curve segments (called *junctions*) must be provided by the user. As illustrated in Fig. 15, different definitions can be considered for junctions, which results in different MAs.

Fortunately, in case of rivers, junctions of river networks are well-defined (i.e., the intersection of two river segments), so automatic tools could be deployed for river network sampling. For a proper sampling, all junctions should be sampled. Then, enough points on each river segment are sampled so that a fair approximation of the river shape is provided. We used "geometric network" extension of the ArcGIS software to automatically extract the junctions. Then, each river segment is sampled using the "line-to-point" tool, which automatically samples a river network and assigns the attributes (including the ID) of that river segment to all of its corresponding sample points.

4.2. Improved one-step crust and skeleton algorithm through labeling sample points

In the following, we propose an improvement to the one-step crust and skeleton algorithm through labeling the sample points in order to automatically avoid appearing extraneous branches in the MA, and show how the proposed method improves the results (Ghandehari and Karimipour, 2012; Karimipour and Ghandehari, 2012).

Fig. 16a illustrates the MA of a shape extracted using the OSCS algorithm. As this figure shows, this algorithm detects some extraneous MA edges, which are filtered through simplification or pruning. We observed that such extraneous edges are the Voronoi edges created between the sample points that lie on the same segment of the curve. It led us to the idea of labeling the sample points in order to automatically avoid appearing such edges in the MA (Fig. 16b).

We consider the shape as different curve segments $\partial\mathcal{O}_i$ such that:

$$\partial\mathcal{O} = \bigcup_{i=1}^{n} \partial\mathcal{O}_i \tag{3}$$

Inner and outer Voronoi edges do not intersect with $\partial\mathcal{O}$, but mixed Voronoi edges do (Giesen et al., 2007). The same applied to the Delaunay edges: Delaunay edges of the sample points S are classified into three classes: *Mixed Delaunay edges* that join two consecutive points and belong to the crust; and *inner/outer Delaunay edges* that join two non-consecutive points and are completely inside/outside $\mathcal{O}$ (all Delaunay vertices lie on the $\partial\mathcal{O}$). Note that the inner/outer/mixed Voronoi edges are dual to the inner/outer/mixed Delaunay edges.

Based on the above definitions, the extraneous MA edges are the inner Voronoi edges that the vertices of their dual Delaunay edges lie on the same curve segment; And, the main MA edges are the inner Voronoi edges that the vertices of their dual Delaunay edges lie on two different curve segments. Therefore, the main

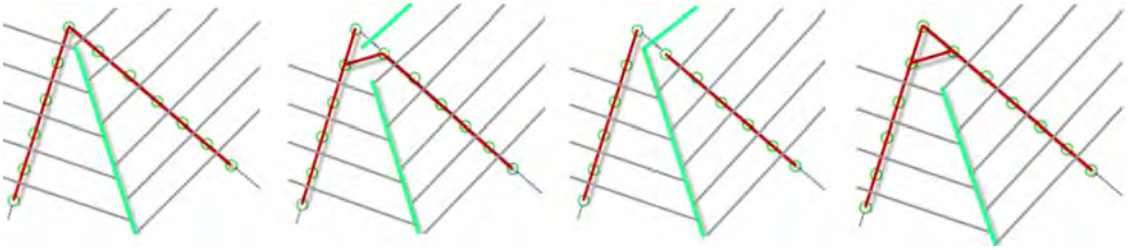

Fig. 18. Different states that may occur at sharp corners. The MA (green) has broken into the curve (red). (For interpretation of the references to color in this figure legend, the reader is referred to the web version of this article.)

idea of the improved method is to remove all the MA edges whose corresponding Delaunay edges lie on the same boundary curve.

To apply our algorithm, the sample points must be labeled: All junctions are assigned *JNC* as label. All of the points sampled on each river segment are already assigned the unique label (ID) of that segment during the sampling process (see Section 4.1)

Filtering in the proposed method is not a pre- or post-processing step, but it is performed, simultaneously, with the MA extraction. To extract the MA, we use the OSCS algorithm. The *InCircle* test is applied on all Delaunay edge: If the determinant is negative and the corresponding Delaunay vertices have the same labels or one of them is a junction, that Delaunay edge is part of the crust. Otherwise, if the determinant is positive and the corresponding Delaunay vertices have different labels, its dual is added to the MA.

To apply the proposed improvement in the OSCS algorithm, the lines 8 and 9 of the pseudo-code presented in Section 3.1 are modified as follows:

8. If $H<0$ and ($L(D_1)=L(D_2)$ or ($L(D_1)=JNC$ or $L(D_2)=JNC$)) then $D_1D_2\in$Crust
9. else if $H>0$ and $L(D_1)\sim=L(D_2)$ then $V_1V_2\in$Skeleton

where $L(D_i)$ means the label of the vertex D_i. Fig. 17 illustrates the result of using the proposed method to extract the MA of the river network presented in Fig. 5, in which the extraneous branches are automatically avoided.

4.3. Handling sharp corners

If the MA is very close to the samples, which is the case at sharp corners, the OSCS algorithm may not reconstruct the original curves (the rivers, in our case) if the sample points does not equally distributed. It results in breaking the MA through the curves (Fig. 18). Based on the sampling theories, infinite density sampling is needed to guarantee the correct reconstruction, which

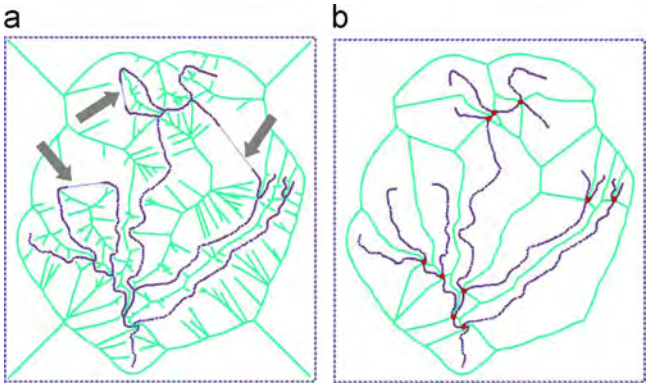

Fig. 20. The MA extraction for open curves when two line segments have the same direction: (a) OSCS algorithm (arrows show mistakenly connected rivers); (b) the proposed algorithm.

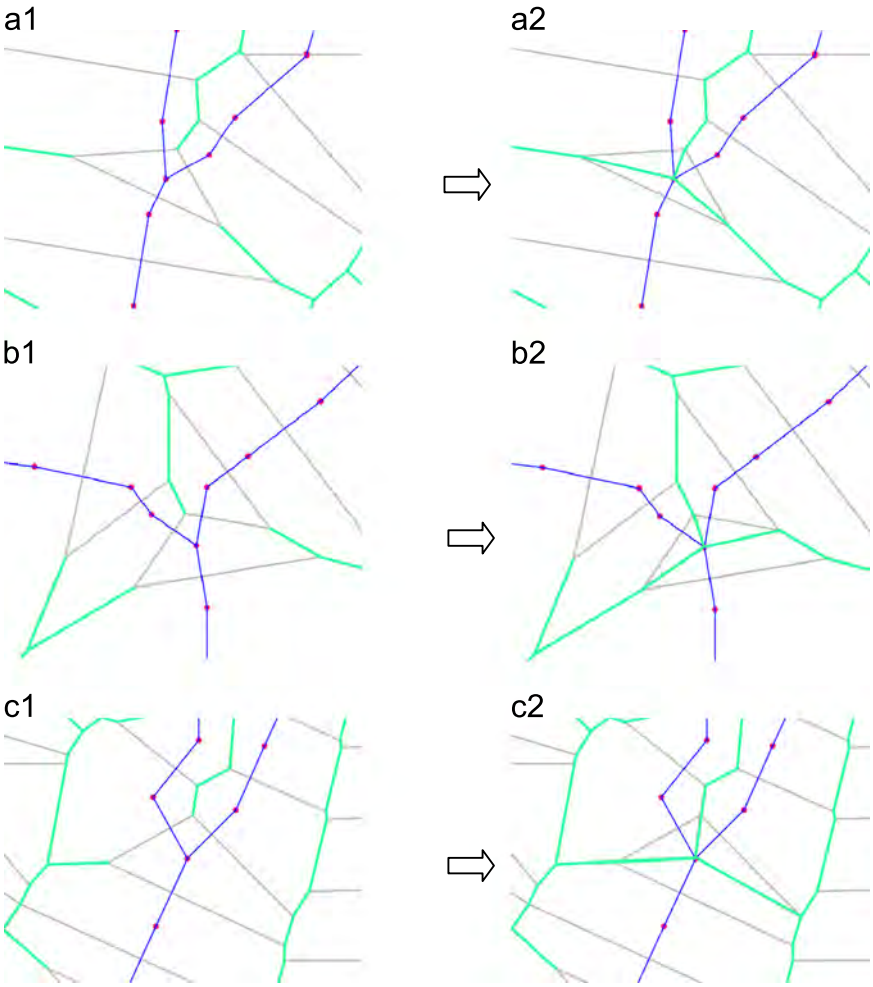

Fig. 19. Different configuration of the MA (green lines) around the junctions: (left) before correction; (right) after correction. (For interpretation of the references to color in this figure legend, the reader is referred to the web version of this article.)

is not practically possible. Instead, the user must check manually the entire MA and manually correct the reconstructed curve, which is time-consuming for high volume data.

Here, we detect the problematic shape corners through a post-processing step: After curve reconstruction, the number of lines joined at each junction is counted, and the corners for which this number is less than a threshold are considered as problematic (in case of rivers, this threshold is practically 3, assuming that a river network will never split to more than two channels). Finally, the sample points around the problematic corners are randomly moved a bit.

4.4. Closing the polygons

The computed MA is a set of lines, whose union does not necessarily construct a closed polygon (catchment, here) for each curve segment (river, here), so the user must manually close the polygons. Here, we connect each junction to three of the vertices of the Voronoi cell that containing that junction, depending on the configuration of the MA around the junction (again, note that we assume that a river network will never split to more than two channels):

- The Voronoi cell of the junction point is a triangle (Fig. 19a1). Here, the three vertices of the Voronoi cell are connected to the junction point (Fig. 19a2).
- The Voronoi cell of the junction point has more than three vertices, and k of these vertices are dangle nodes (i.e., nodes that are connected to only one line segment). If $k=3$ (Fig. 19b1), the three dangle vertices are connected to the junction point (Fig. 19b2). Otherwise, if $k<3$ (Fig. 19c1), the k dangle nodes plus $3-k$ random vertices are connected to the junction (Fig. 19c2).

4.5. Open curves

The Vornoi-based MA extraction algorithms are designed to extract the MA of closed curves, which is not the case with the river networks. Thus, applying the MA extraction algorithm to river networks does not produce the expected results in some cases, which must be edited by the user. As illustrated in Fig. 20a, if two distinct river branches are collinear, they are mistakenly connected as a single curve at the curve reconstruction step, and consequently, no MA edge is drawn between them. In the proposed method, such problems are automatically avoided, because, as described, the crust edge is not drawn between two sample points with different labels.

4.6. Twisted polygons

Since the proposed method uses the vector data of the rivers, no raster to vector conversion is performed at the end, hence the problem of the twisted polygons does not happen (Fig. 21).

4.7. Hierarchical delineation

The MA extracted for a river network has the form of a set of polygons (called catchment polygons) each of which corresponds to a river segment. Merging the polygons extracted for the river segments falls into the same main river yields the watersheds. In raster-based algorithm, the watershed for any point in the network can be determined by following the network upstream from that point and merging the related catchment polygons. In the proposed method, we assign a distinct label to the sample points of each river. On the other hand, each main river is assigned a code; then all rivers fall into the same main river are assigned the code of that main river as the second label. If the first labels are used for the MA extraction, the catchments are extracted, while MA extraction using the second labels will directly provide the watersheds (Fig. 22).

5. Results and discussion

This section presents the results of watershed delineation for four case studies using the proposed approach and compares the results with the watersheds delineated using a DEM-based method.

The study areas are Denton, Hondo, Middle Colorado and San Marcos basins all located in the Texas State, USA (Fig. 23). The area as well as the number of hydrologic units (i.e., watersheds, subwatersheds and catchments) of each basin is presented in Table 1. The data used here consists of rivers data from the NHDPlus, which are the National Hydrography Dataset (NHD) improved by the Horizon Systems Corporation.

The hydrologic units for the basins were obtained from NHDPlus. As example, Fig. 24 shows these units for the San Marcos basin.

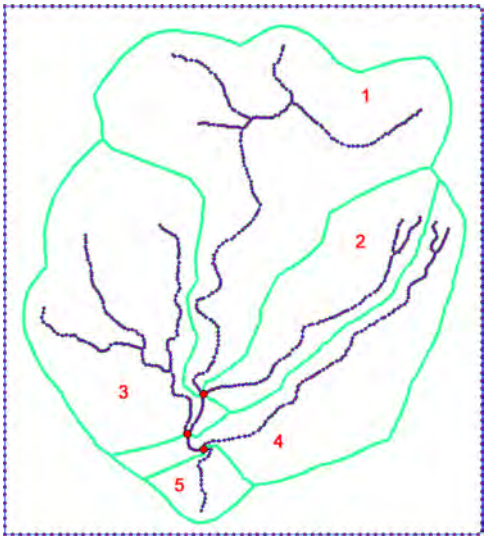

Fig. 22. Watersheds delineated using the proposed methods.

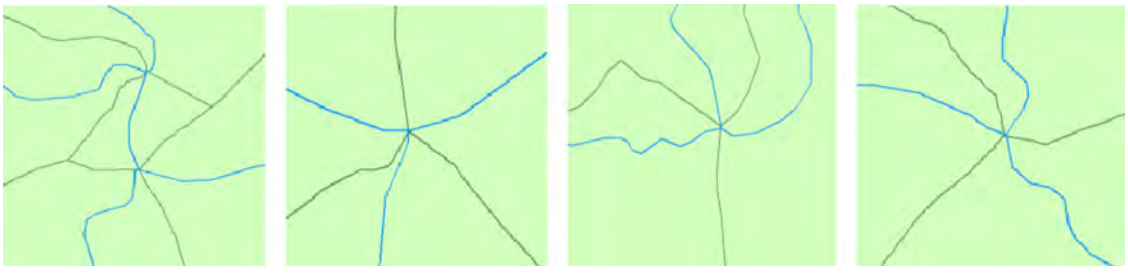

Fig. 21. The catchments (green lines) delineated using the proposed method for the rivers (blue lines) presented in Fig. 1 where DEM-based methods caused twisted polygons. (For interpretation of the references to color in this figure legend, the reader is referred to the web version of this article.)

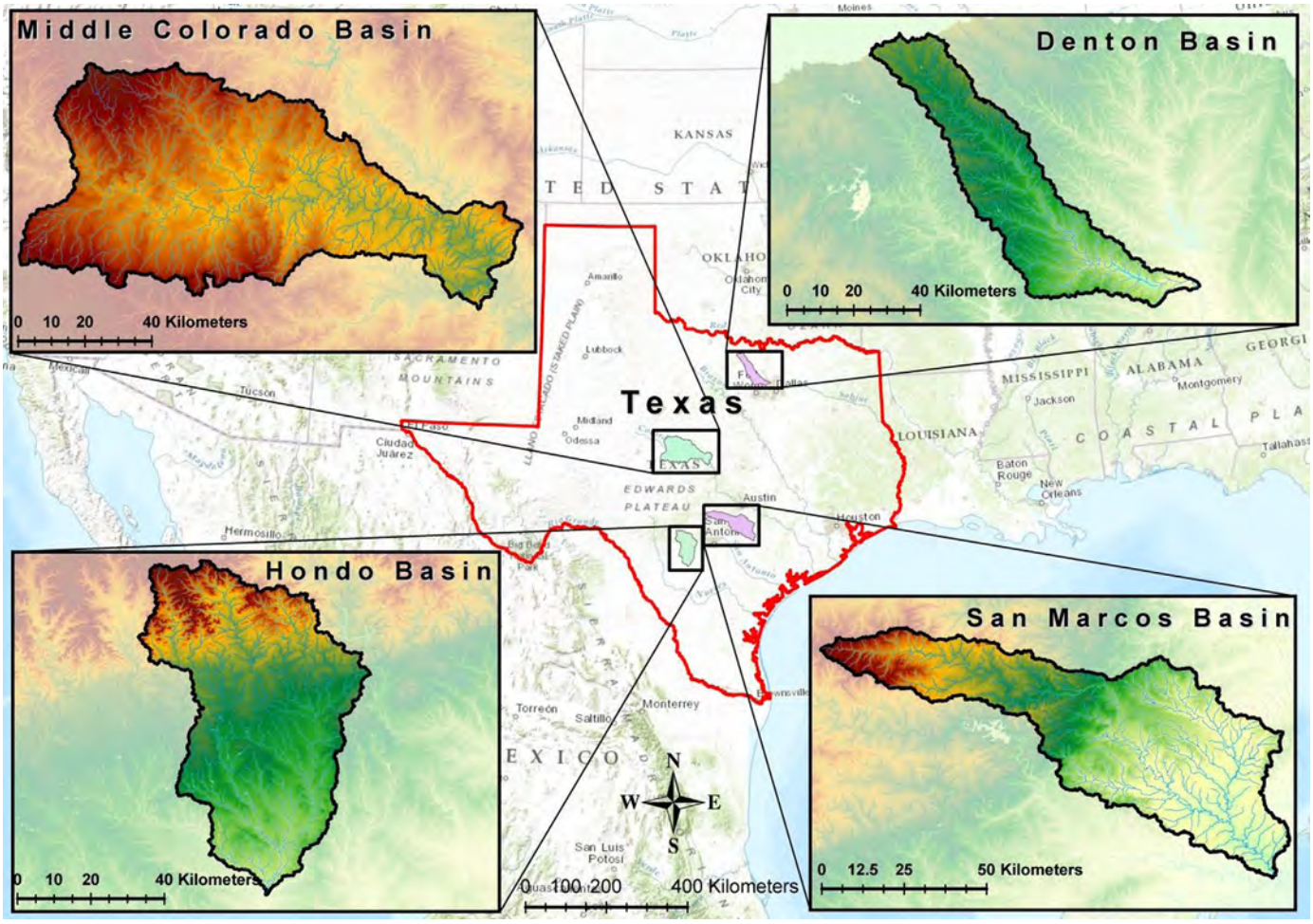

Fig. 23. Study areas located in the Texas state.

Table 1
Area and number of hydrological units of the four case studies.

Basin	Area (km^2)	No. of catchments	No. of subwatersheds	No. of watersheds
Denton	1863.3	447	18	3
Hondo	2867.6	359	27	4
M. Colorado	5213.6	604	44	6
San Marcos	3528.8	369	32	9

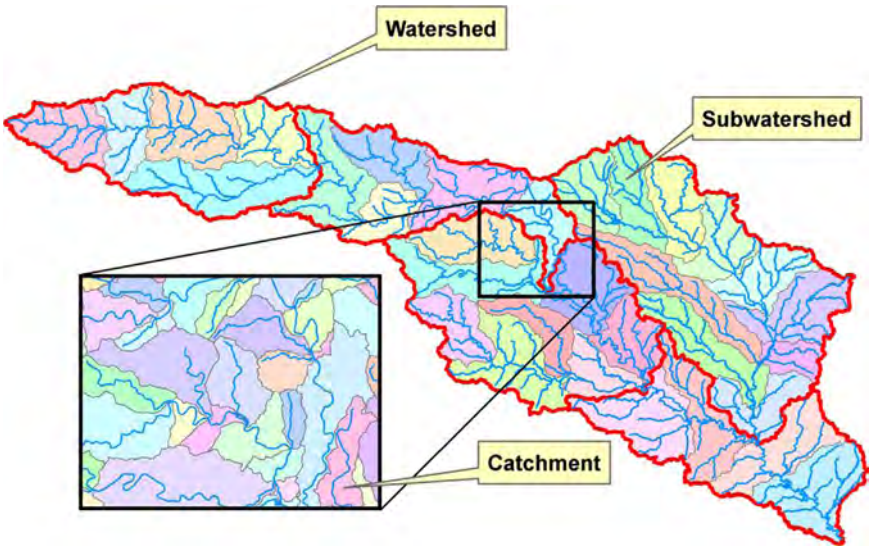

Fig. 24. Hydrologic units of San Marcos basin: catchments, subwatersheds and watersheds.

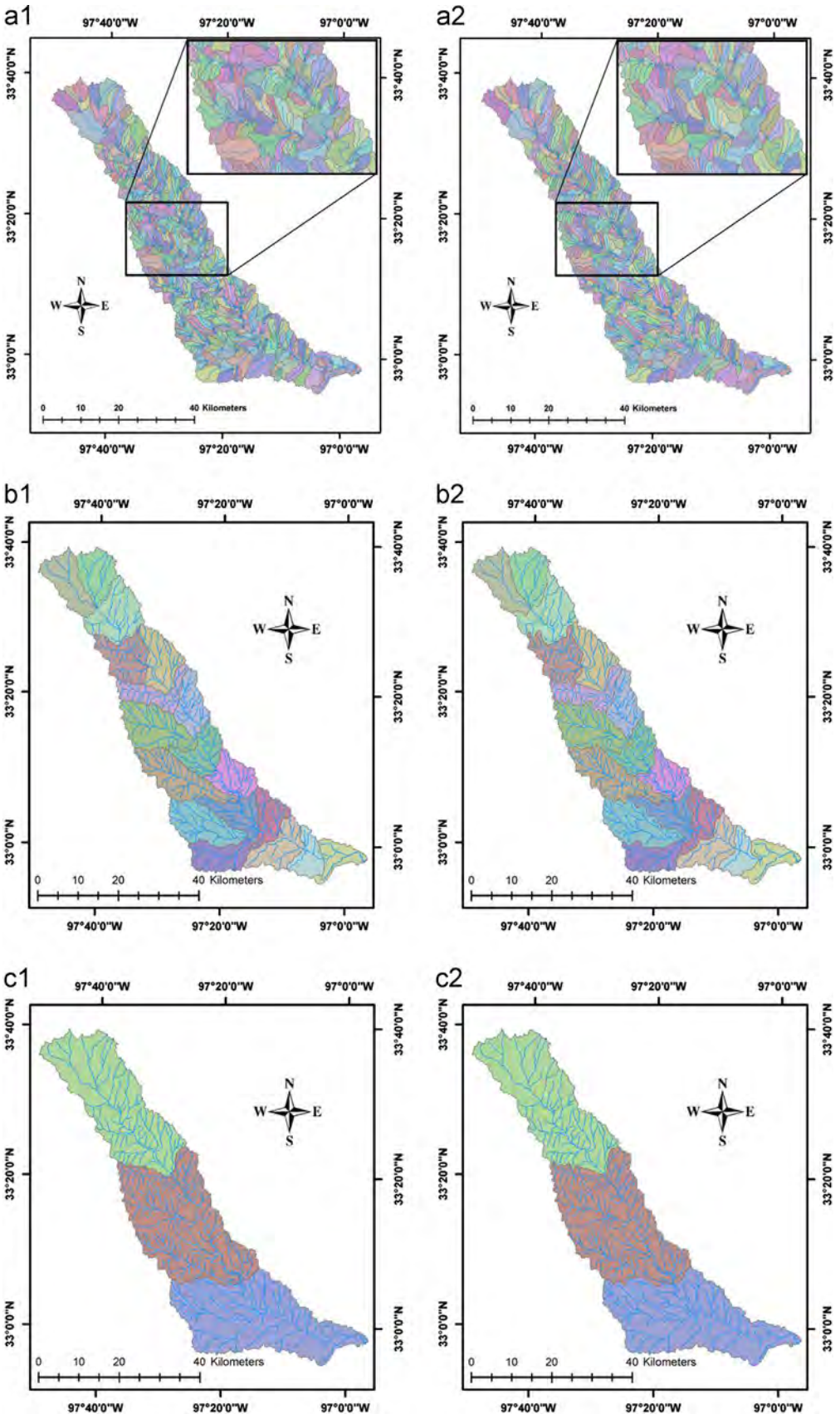

Fig. 25. Catchments ((a1) and (a2)), subwatersheds ((b1) and (b2)) and watersheds ((c1) and (c2)) of the Denton basin provided by NHDPlus (left) and the proposed method (right).

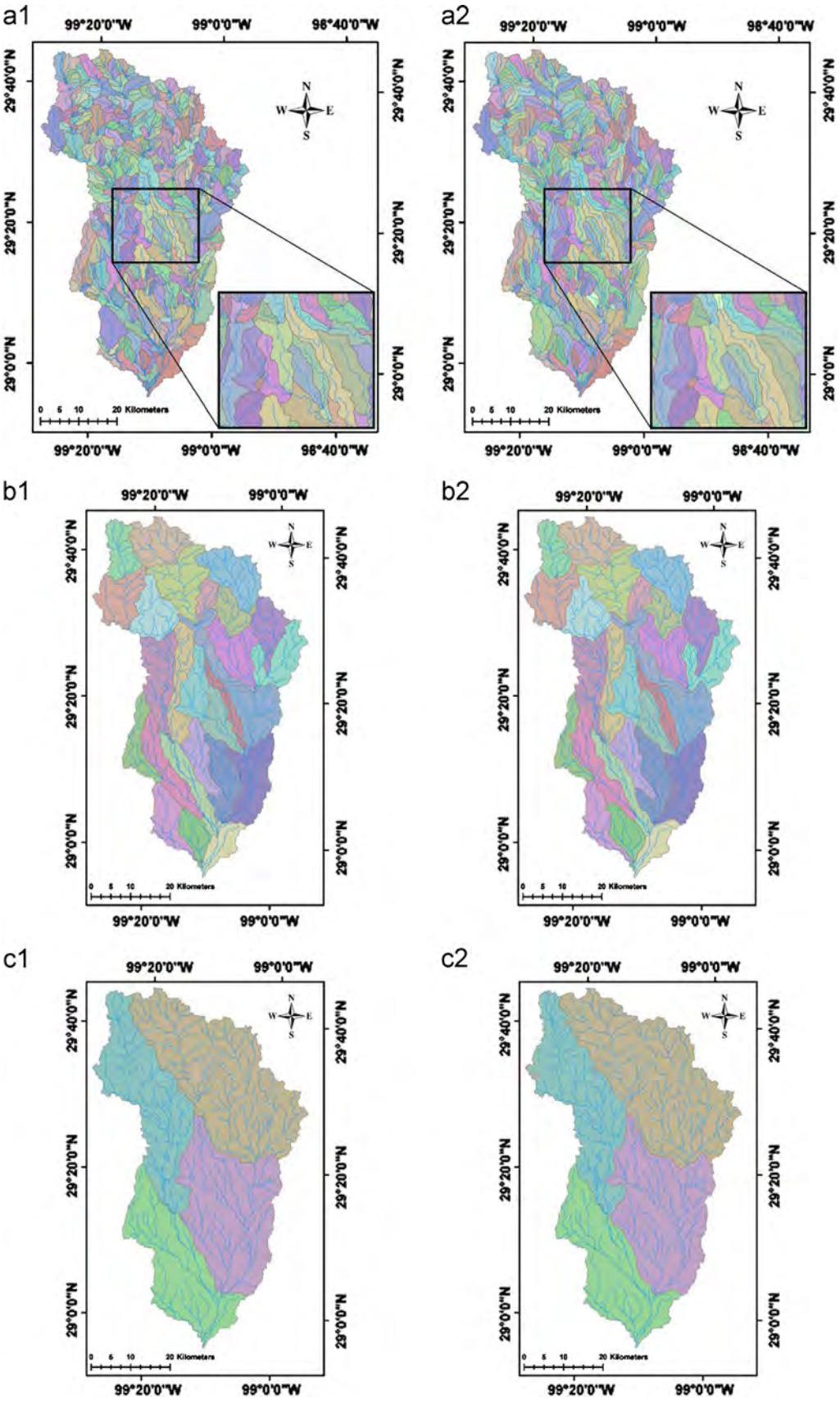

Fig. 26. Catchments ((a1) and (a2)), subwatersheds ((b1) and (b2)) and watersheds ((c1) and (c2)) of the Hondo basin provided by NHDPlus (left) and the proposed method (right).

They will be used for accuracy assessment as reference data in Section 5.2.

Figs. 25–28 illustrate the catchments, subwatersheds and watersheds delineated for the case studies using the proposed approach.

5.1. Efficiency

The watershed delineation is a time-consuming analysis. Although numerous studies have been done to improve the accuracy of the watershed delineation, there have been a few attempts for increasing the efficiency of these methods. The time consumption of the raster-based algorithms depends on the number of cells (which is a function of the size of the region and the grid cell size). We use only the river networks for the watershed delineation, which is a much smaller dataset comparing DEM, so the algorithm is much faster. The proposed approach performs Delaunay triangulation in $O(n\log n)$ time, where n is the number of sample points. Extraction of Voronoi diagram from Delaunay triangulation as well as OSCS algorithm take linear time. Thus, complexity of the proposed approach is $O(n\log n)$.

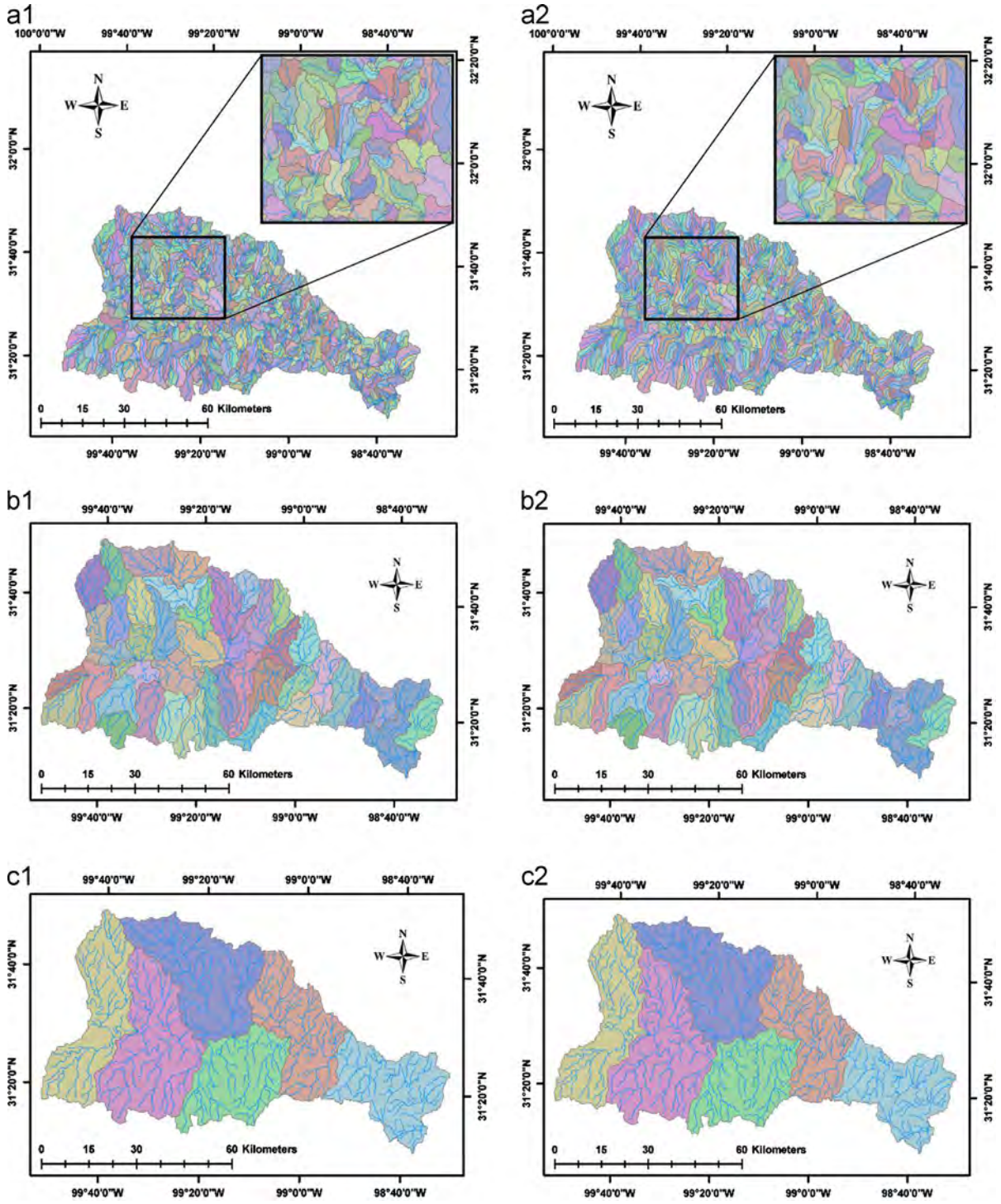

Fig. 27. Catchments ((a1) and (a2)), subwatersheds ((b1) and (b2)) and watersheds ((c1) and (c2)) of the middle Colorado basin provided by NHDPlus (left) and the proposed method (right).

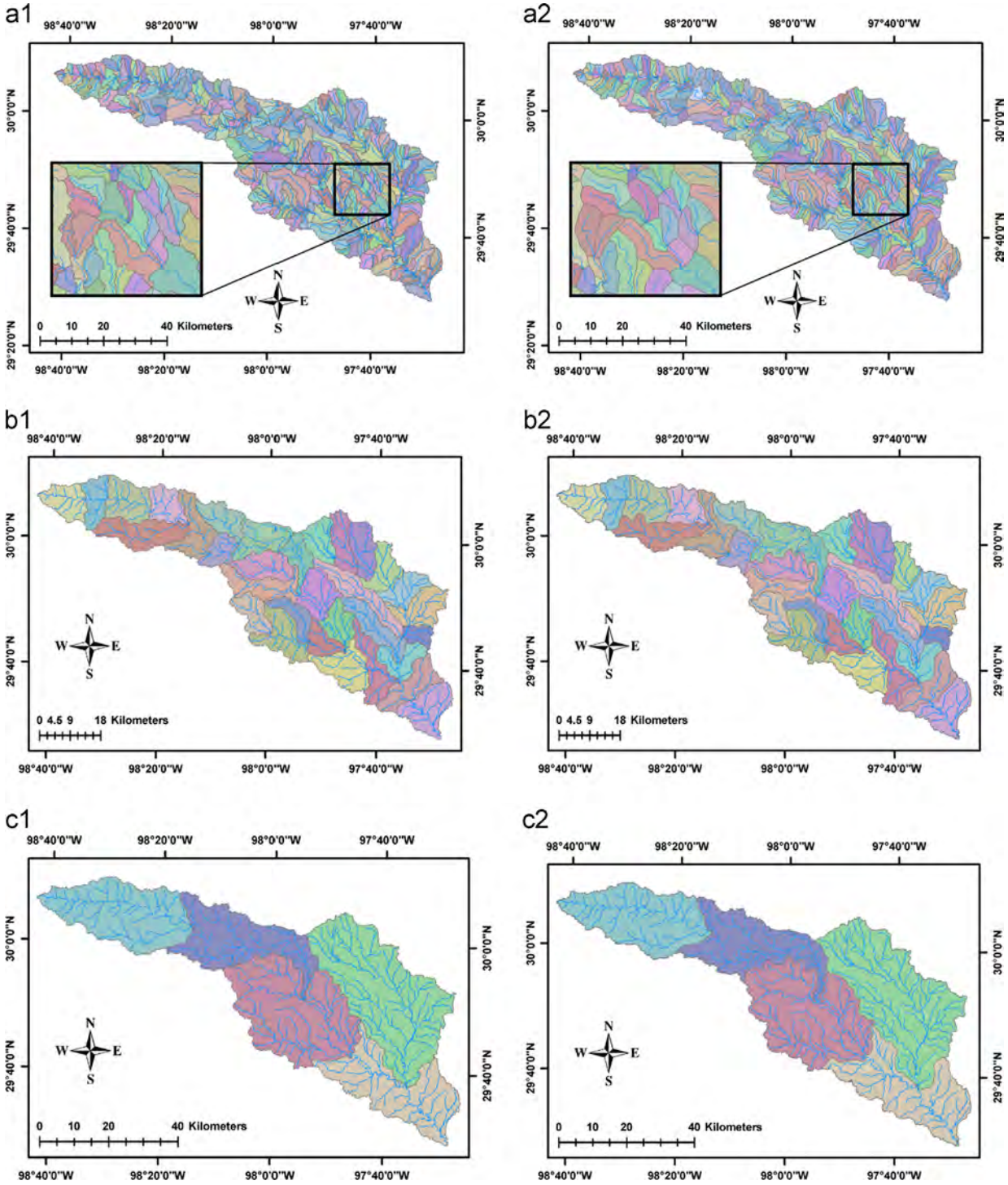

Fig. 28. Catchments, subwatersheds and watersheds of the San Marcos basin provided by NHDPlus (left) and the proposed method (right).

5.2. Accuracy assessment

To assess the accuracy of the results, we consider the hydrologic units obtained from NHDPlus as reference data and check the agreement between this reference data and the results of the proposed approach. For this, the idea of error matrix (i.e., a common tool to evaluate the classification accuracy of remotely sensed data) was imitated. First, each reference layer was intersected with the corresponding result, which produces lots of polygons (Fig. 29). Each polygon in the new intersected layer is assigned two labels respect to the ID of the polygons in the input layers. Thus, the error matrix is an array of size $k \times k$ (where k is the number polygons in the intersected layer). The rows and columns, respectively, represent the results and the reference data; and the cell values refer to the area size of the corresponding polygons. The diagonal elements indicate the area of the polygons correctly delineated (have the same labels), whereas the off-diagonal elements contain those polygons with different labels.

Two quantitative parameters namely the overall accuracy and the kappa coefficient (K) were also computed from the error matrix: The overall accuracy is the total area of correctly delineated watersheds (i.e., sum of all major diagonal elements) divided by the total

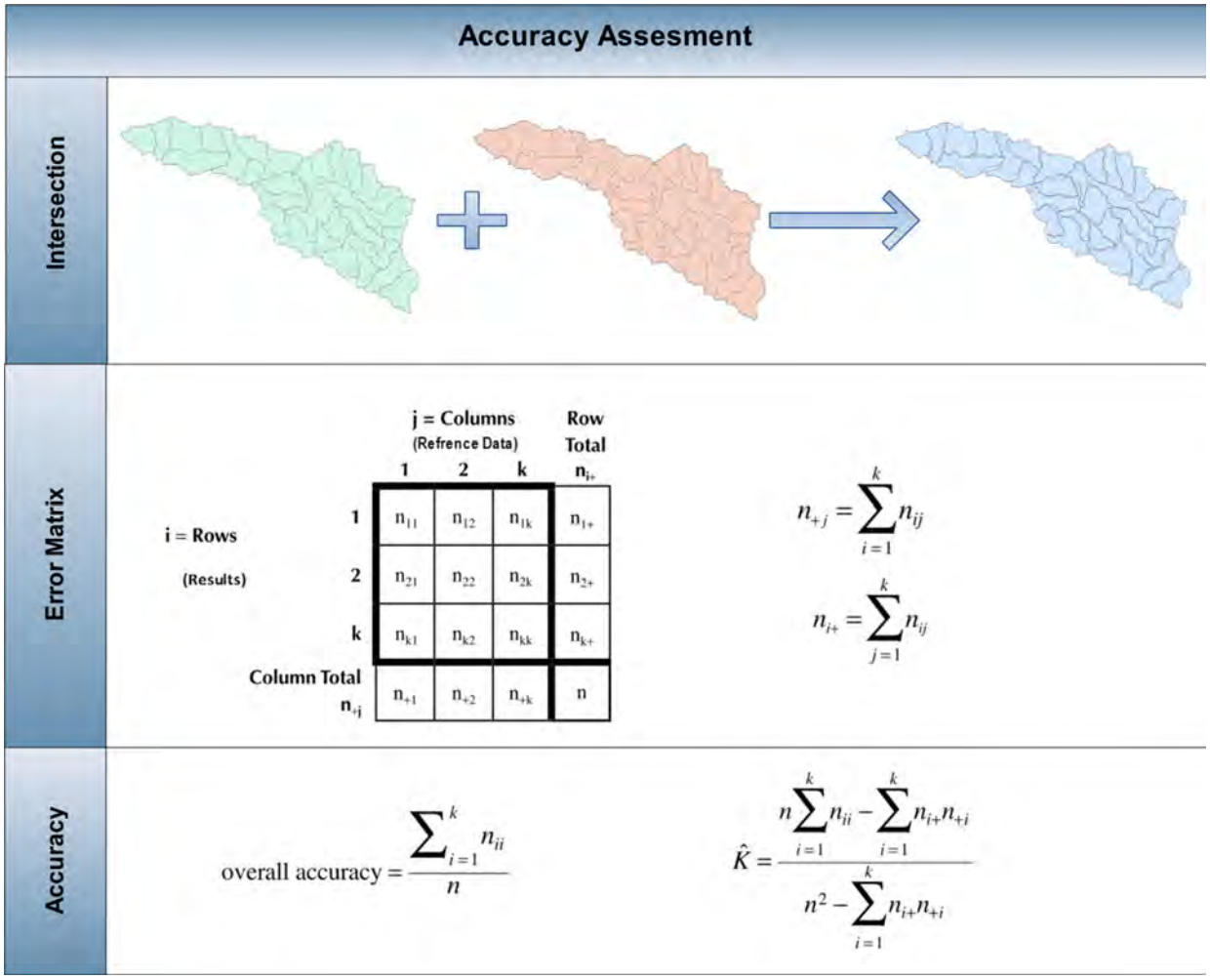

Fig. 29. Accuracy assessment procedure using the error matrix.

Table 2
Overall accuracy and kappa coefficient of the results produced for the case studies using the proposed method.

Basin	Catchment		Subwatershed		Watershed	
	Overall accuracy (%)	Kappa (%)	Overall accuracy (%)	Kappa (%)	Overall accuracy (%)	Kappa (%)
Denton	76.95	76.83	94.66	94.33	99.33	98.99
Hondo	76.59	76.46	92.09	91.76	97.86	97.09
M. Colorado	78.02	77.96	92.18	91.98	98.07	97.67
San Marcos	77.46	77.34	92.00	91.72	97.75	97.01

area of study area (i.e., total sum of all elements of the table). Kappa coefficient is another measure of accuracy defined as the difference between the actual agreement in the error matrix (indicated by the major diagonal elements) and the chance agreement (indicated by the off-diagonal elements).

The overall accuracy and kappa coefficient of the results for the case studies are illustrated in Table 2. The results show that the accuracy of the proposed method is reasonably comparable to the NHDPlus data, especially for larger hydrologic units (i.e., subwatersheds and watersheds). The reason that larger units compare more favourably than smaller units is that the difference between the proposed method and NHDPlus data happens on the border of the hydrological units. Thus, larger units have more common region and results in less difference. The key point is that at every unit size, our algorithm compares favourably against the reference.

6. Conclusion and future work

This article used the medial axis of river networks as an approximation of the watersheds. The results showed that if an accurate DEM is not available, the river networks can provide a fair approximation of the watersheds. However, there are a few issues to be solved by the medial axis extraction algorithms in order to be practically used for watershed delineation from river networks: (1) They are prone to perturbations caused by sampling; (2) they have problems in the medial axis extraction at sharp corners; (3) they are not designed to be applied on open curves (the rivers, here); and (4) they does not necessarily produce closed polygons (catchments, here). We proposed an approach that consider all the issues and explained how to produce the watersheds from the river networks. The core of the approach was improving a medial

axis extraction method (one-step crust and skeleton algorithm) by labeling the sample points to automatically avoid appearing extraneous branches in the medial axis. The results of the case studies illustrated that the approach provides a fair approximation of the hydrological units, especially for subwatersheds and watersheds.

Sampling of a river network is a straightforward task as junctions of river networks are well-defined (i.e., the intersection of two river segments), so automatic tools could be deployed for river network sampling. In general, however, sampling is performed manually due to the fact that junctions must be provided by the user. We are working on a semi-automatic process that only the junctions are manually sampled, between which enough points – to fairly approximate the curve – are automatically sampled and labeled through an initial curve reconstruction. Finally, extending the improved crust and MA extraction method to 3D objects is a direction for future work.

Acknowledgments

We would like to deeply appreciate Richard Barnes, University of Minnesota for his invaluable constructive comments on the article.

References

Al-Muqdadi, S.W., Merkel, B.J., 2011. Automated watershed evaluation of flat terrain. Journal of Water Resource and Protection 3, 892–903, http://dx.doi.org/10.4236/jwarp.2011.312099.

Amenta, N., Bern, M.W., Eppstein, D., 1998. The crust and the beta-skeleton: combinatorial curve reconstruction. Graphical Models and Image Processing 60, 125–135, http://dx.doi.org/10.1006/gmip.1998.0465.

Amenta, N., Choi, S., Kolluri, R.K., 2001. The power crust. In: Proceedings of the Sixth ACM Symposium on Solid Modeling and Applications, pp. 249–266. http://dx.doi.org/10.1145/376957.376986.

Amenta, N., Kolluri, R.K., 2001. The medial axis of a union of balls. Computational Geometry 20, 25–37, http://dx.doi.org/10.1016/S0925-7721(01)00033-5.

Attali, D., di Baja, G., Thiel, E., 1995. Pruning discrete and semicontinuous skeletons. Image Analysis and Processing, 488–493, http://dx.doi.org/10.1007/3–540-60298-4_303.

Attali, D., Montanvert, A., 1994. Semicontinuous skeletons of 2D and 3D shapes. Aspects of Visual Form Processing, 32–41.

Attali, D., Montanvert, A., 1996. Modeling noise for a better simplification of skeletons. In: International Conference on Image Processing, pp. 13–16. http://dx.doi.org/10.1109/ICIP.1996.560357.

Attali, D., Montanvert, A., 1997. Computing and simplifying 2D and 3D continuous skeletons. Computer Vision and Image Understanding 67, 261–273, http://dx.doi.org/10.1006/cviu.1997.0536.

Aurenhammer, F., 1991. Voronoi diagrams—a survey of a fundamental geometric data structure. ACM Computing Surveys 23, 345–405, http://dx.doi.org/10.1145/116873.116880.

Bai, X., Latecki, L., 2007. Discrete skeleton evolution. Energy Minimization Methods in Computer Vision and Pattern Recognition, pp. 362–374, http://dx.doi.org/10.1007/978-3-540-74198-5_28.

Blum, H., et al., 1967. A transformation for extracting new descriptors of shape. 19. Models for the Perception of Speech and Visual Form, pp. 362–380.

Chazal, F., Lieutier, A., 2005. The “Lambda medial axis”. Graphical Models 67, 304–331, http://dx.doi.org/10.1016/j.gmod.2005.01.002.

Cheng, S.W., Funke, S., Golin, M., Kumar, P., Poon, S.H., Ramos, E., 2005. Curve reconstruction from noisy samples. Computational Geometry 31, 63–100, http://dx.doi.org/10.1016/j.comgeo.2004.07.004.

Chorowicz, J., Ichoku, C., Riazanoff, S., Kim, Y.J., Cervelle, B., 1992. A combined algorithm for automated drainage network extraction. Water Resources Research 28, 1293–1302, http://dx.doi.org/10.1029/91WR03098.

Delaunay, B., 1934. Sur la sphere vide. Izv. Akad. Nauk SSSR, Otdelenie Matematicheskii i Estestvennyka Nauk 7, 793–800.

Dey, T.K., Wenger, R., 2002. Fast reconstruction of curves with sharp corners. International Journal of Computational Geometry and Applications 12, 353–-400, http://dx.doi.org/10.1142/S0218195902000931.

Dillabaugh, C., 2002. Drainage basin delineation from vector drainage networks. In: Symposium on Geospatial Theory, Processing and Applications. Ottawa, Ontario, Canada.

Ghandehari, M., Karimipour, F., 2012. Voronoi-based curve reconstruction: issus and solutions. In: al., B.M.e. (Ed.), The International Conference on Computational Science and Its Applications (ICCSA 2012). Springer-Verlag, Salvador de Bahia, Brazil, pp. 194–207. http://dx.doi.org/10.1007/978-3-642-31075-1_15.

Giesen, J., Miklos, B., Pauly, M., 2007. Medial axis approximation of planar shapes from union of balls: a simpler and more robust algorithm. In: Canadian Conference. Computational Geometry, pp. 105–108.

Giesen, J., Miklos, B., Pauly, M., Wormser, C., 2009. The scale axis transform. In: Proceedings of the 25th Annual Symposium on Computational Geometry, pp. 106–115. http://dx.doi.org/10.1145/1542362.1542388.

Gold, C., Dakowicz, M., 2005. The crust and skeleton–applications in GIS. In: Proceedings of Second International Symposium on Voronoi Diagrams in Science and Engineering, pp. 33–42.

Gold, C., Snoeyink, J., 2001. A one-step crust and skeleton extraction algorithm. Algorithmica 30, 144–163, http://dx.doi.org/10.1007/s00453-001-0014-x.

Gonzalez, R.C., Woods, R.E., 2002. Digital Image Processing. Pearson Education, Prentice Hall, USA.

Jones, N.L., Wright, S.G., et al., 1990. Watershed delineation with triangle-based Terrain models. Journal of Hydraulic Engineering 116, 1232, http://dx.doi.org/10.1061/(ASCE)0733-9429(1990)116:10(1232).

Karimipour, F., Delavar, M.R., Frank, A.U., 2008. A mathematical tool to extend 2D spatial operations to higher dimensions. In: Gervasi, O., Murgante, B., Lagana, A., Taniar, D., Mun, Y., Gavrilova, M. (Eds.), The International Conference on Computational Science and Its Applications (ICCSA 2008). Springer-Verlag, Perugia, Italy, pp. 153-167. http://dx.doi.org/10.1007/978-3-540-69839-5_12

Karimipour, F., Delavar, M.R., Frank, A.U., 2010. A simplex-based approach to implement dimension independent spatial analyses. Computers & Geosciences 36, 1123–1134, http://dx.doi.org/10.1016/j.cageo.2010.03.002.

Karimipour, F., Ghandehari, M., 2012. A stable Voronoi-based algorithm for medial axis extraction through labeling sample points. In: Proceedings of the Ninth International Symposium on Voronoi Diagrams in Science and Engineering (ISVD 2012). New Jersey, USA. http://dx.doi.org/10.1109/ISVD.2012.20.

Karimipour, F., Ghandehari, M., 2013. Accepted to be published in ‘Voronoi-based medial axis approximation from samples: issues and solutions. Transactions on Computational Science.

Ledoux, H., 2006. Modelling Three-dimensional Fields in Geo-Science with the Voronoi Diagram and its Dual. Ph.D. Dissertation. School of Computing, University of Glamorgan, Pontypridd, Wales, UK.

Ledoux, H., Gold, C.M., 2007. Simultaneous storage of primal and dual three-dimensional subdivisions. Computers, Environment and Urban Systems 31, 393–408, http://dx.doi.org/10.1016/j.compenvurbsys.2006.03.003.

Li, Z., Zhu, C., Gold, C., 2005. Digital Terrain Modeling: Principles and Methodology. CRC Press, USA.

Lin, W.T., Chou, W.C., Lin, C.Y., Huang, P.H., Tsai, J.S., 2006. Automated suitable drainage network extraction from digital elevation models in Taiwan's upstream watersheds. Hydrological Processes20, 289–306, http://dx.doi.org/10.1002/hyp.5911.

Malandain, G., Fernández-Vidal, S., 1998. Euclidean skeletons. Image and Vision Computing 16, 317–327, http://dx.doi.org/10.1016/S0262-8856(97)00074-7.

Mark, D.M., 1984. Part 4: Mathematical, algorithmic and data structure issues: automated detection of drainage networks from digital elevation models. Cartographica: The International Journal for Geographic Information and Geovisualization 21, 168–178, http://dx.doi.org/10.3138/10LM-4435-6310-251R.

Martz, L.W., Garbrecht, J., 1992. Numerical definition of drainage network and subcatchment areas from digital elevation models. Computers & Geosciences 18, 747–761, http://dx.doi.org/10.1016/0098-3004(92)90007-E.

Martz, L.W., Garbrecht, J., 1993. Automated extraction of drainage network and watershed data from digital elevation models. JAWRA Journal of the American Water Resources Association 29, 901–908, http://dx.doi.org/10.1111/j.1752-1688.1993.tb03250.x.

McAllister, M., 1999. The Computational Geometry of Hydrology Data in Geographic Information System. Ph.D. Dissertation. University of British Columbia.

Miklós, B., 2012. Mesecina, ETH Zurich, p. ⟨http://www.balintmiklos.com/mesecina⟩.

Mostafavi, M.A., Gold, C., Dakowiczb, M., 2003. Delete and insert operations in Voronoi/Delaunay: methods and applications. Computers & Geosciences 29, 523–530, http://dx.doi.org/10.1016/S0098-3004(03)00017-7.

Mower, J.E., 1994. Data-parallel procedures for drainage basin analysis. Computers & Geosciences 20, 1365–1378, http://dx.doi.org/10.1016/0098-3004(94)90060-4.

Nelson, E., Jones, N., Miller, A., 1994. Algorithm for precise drainage-basin delineation. Journal of Hydraulic Engineering 120, 298, http://dx.doi.org/10.1061/(ASCE)0733-9429(1994)120:3(298).

Ogniewicz, R.L., Kübler, O., 1995. Hierarchic Voronoi skeletons. Pattern Recognition 28, 343–359, http://dx.doi.org/10.1016/0031-3203(94)00105-U.

Okabe, A., Boots, B., Sugihara, K., Chiu, S.N., 2000. Spatial Tessellations: Concepts and Applications of Voronoi Diagrams, second ed. John Wileyhttp://dx.doi.org/10.1002/9780470317013.

Russ, J.C., 2002. The Image Processing Handbook. CRC Pr.http://dx.doi.org/10.1201/9781420040760.

Siddiqi, K., Bouix, S., Tannenbaum, A., Zucker, S.W., 2002. Hamilton-jacobi skeletons. International Journal of Computer Vision 48, 215–231.

Tarboton, D.G., 1997. A new method for the determination of flow directions and upslope areas in grid digital elevation models. Water Resources Research 33, 309–319, http://dx.doi.org/10.1029/96WR03137.

Turcotte, R., Fortin, J.P., Rousseau, A., Massicotte, S., Villeneuve, J.P., 2001. Determination of the drainage structure of a watershed using a digital elevation model and a digital river and lake network. Journal of Hydrology 240, 225–242, http://dx.doi.org/10.1016/S0022-1694(00)00342-5.

Yang, W., Hou, K., Yu, F., Liu, Z., Sun, T., 2010. A novel algorithm with heuristic information for extracting drainage networks from raster DEMs. Hydrology Earth System Science Discussions 7, 441–459, http://dx.doi.org/10.5194/hessd-7-441-2010.